Annali di Matematica Pura ed Applicata (1923 -) (2019) 198:727–747
https://doi.org/10.1007/s10231-018-0795-z

Heegaard splittings of graph manifolds

Enrique Artal Bartolo[1] · **Simón Isaza Peñaloza**[2] · **Miguel Á. Marco-Buzunáriz**[1]

Received: 20 March 2018 / Accepted: 26 September 2018 / Published online: 4 October 2018

Abstract
In this paper, we give a method to construct Heegaard splittings of oriented graph manifolds with orientable bases. A graph manifold is a closed 3-manifold admitting only Seifert-fibered pieces in its Jaco–Shalen–Johansson decomposition; for technical reasons, we restrict our attention to the *fully* oriented case, i.e., when both the pieces and the bases are oriented.

Keywords Heegaard splittings · Graph manifolds · Plumbing calculus

Mathematics Subject Classification Primary 57N10; Secondary 57M27

In this paper, we deal with graph manifolds. A closed 3-manifold M is said to be a graph manifold if its Jaco–Shalen–Johansson decomposition admits only Seifert-fibered pieces. These manifolds were classified by Waldhausen [11,12] and are completely determined by a normalized weighted graph (up to a controlled family of exceptions). For technical reasons, we restrict ourselves to the *fully* oriented case, i.e., we assume that M is oriented and that the bases of the Seifert fibrations are oriented surfaces. This is only a mild restriction and this family contains the class of 3-manifolds which appear naturally in complex geometry: boundaries of regular neighborhoods of complex curves in complex surfaces. These manifolds admit yet another classification in terms of plumbing graphs, see the work of Neumann [5].

A *Heegaard splitting* of a closed orientable 3-manifold M is a decomposition of M as a union of two handlebodies sharing a common boundary. This common boundary is a closed

First named author is partially supported by MTM2016-76868-C2-2-P and Grupo "Álgebra y Geometría" of Gobierno de Aragón/Fondo Social Europeo. Second named author is partially supported by MTM2016-76868-C2-1-P. Third named author is partially supported by MTM2016-76868-C2-2-P and Grupo "Investigación en Educación Matemática" of Gobierno de Aragón/Fondo Social Europeo.

✉ Enrique Artal Bartolo
artal@unizar.es

Simón Isaza Peñaloza
psisaza@mat.ucm.es

Miguel Á. Marco-Buzunáriz
mmarco@unizar.es

[1] Departamento de Matemáticas-IUMA, Universidad de Zaragoza, c/Pedro Cerbuna 12, 50009 Saragossa, Spain

[2] Departamento de Álgebra, Universidad Complutense, Plaza de las Ciencias, n. 3, 28040 Madrid, Spain

orientable surface Σ, and the genus of the splitting is defined as the genus of Σ. Given a genus g handlebody, it is possible to take g disks such that, cutting along them, a closed ball is obtained. The boundaries of these g disks provide us with g distinguished curves in the boundary surface. In a Heegaard splitting, since Σ is seen simultaneously as the boundary of two different handlebodies, two families of distinguished curves can be considered. The surface Σ, along with these two families, is called a *Heegaard diagram*, and it determines the manifold M and the splitting itself. Every closed oriented 3-manifold admits a Heegaard splitting, and the *Heegaard genus* of such a manifold is defined as the minimal genus of its Heegaard splittings. See [3] and [8] for details.

There is ample literature about Heegaard splittings of Seifert-fibered manifolds (the *bricks* of graph manifolds), see, e.g. [1,2,4]. In these works, *vertical* and *horizontal* splittings are defined. These ideas were also transferred to the case of graph manifolds in [10], where the structure of Heegaard splittings is studied. In this sense, our approach involves horizontal splittings.

The contribution of this work consists of providing an explicit method to construct a Heegaard diagram of any graph manifold from a plumbing graph presenting it. This method does not provide a splitting of minimal genus. However, from [5], we know a set of moves that can be performed on plumbing graphs without altering the corresponding manifold, and these moves can be used to decrease the genus of the Heegaard splitting given by the method.

Heegaard diagrams were used by Osváth and Szabó [6,7] to define the so-called Heegaard–Floer homology for 3-manifolds. Later Sarkar and Wang in [9] gave an explicit method to compute this homology from Heegaard diagrams. As a future work, our method could be combined with theirs, in order to compute Heegaard–Floer homology for graph manifolds.

The paper is organized as follows. We start by recalling the construction of a graph manifold from its plumbing graph in Sect. 1. We continue in Sect. 2 with the description of the method to construct a Heegaard diagram from a plumbing graph, and its illustration through an example. The rest of the paper is devoted to the proof that the Heegaard diagram thus obtained is in fact a Heegaard diagram for the manifold presented by the graph. In Sect. 3, we provide the main topological constructions that will be needed later, specially the concept of *float gluings*. From this section on, we construct Heegaard splittings and diagrams for increasingly complicated manifolds, until arriving to the general case. In Sect. 4, we construct splittings for $\mathbb{S}^1$-fiber bundles with Euler number ± 1, and the diagram is described. We follow the same structure for general $\mathbb{S}^1$-fiber bundles in Sect. 5. In Sect. 6, we study the splittings of the simplest graph manifolds that are not fibered bundles, i.e., corresponding to a simplicial graph with one edge. The general case is studied in Sect. 7. This stepped procedure allows us to break up the technical difficulties. Finally, in Sect. 8, we provide explicit examples, including a genus 3 splitting of the Poincaré sphere.

1 Plumbing graph of a graph manifold

Graph manifolds [11,12] were defined and classified by Waldhausen and his theory was generalized by Jaco, Shalen and Johansson.

Definition 1.1 An irreducible compact three-manifold is a *graph manifold* if its JSJ-decomposition contains only Seifert pieces.

Waldhausen described these manifolds using a graph where the vertices correspond to the JSJ–Seifert pieces (decorated with the Seifert invariants) and the edges correspond to the

incompressible tori (decorated with the gluing data). For our construction, it is more useful to follow Neumann's approach (*plumbing construction*).

Theorem 1.2 [5, Theorems 5.1 and 5.6] *Any graph manifold can be obtained through the plumbing construction with a unique normal form.*

The rest of the section is devoted to the explicit description of this Neumann's plumbing construction. Since the actual family we are interested in satisfies strong orientation properties, we will restrict ourselves to oriented graph manifolds built up using oriented fibrations.

The main *atoms* in the construction of graph manifolds are $\mathbb{S}^1$-fiber bundles. The oriented $\mathbb{S}^1$-bundles over a manifold N are classified by its Euler class in $H^2(N;\mathbb{Z})$. If N is an oriented closed surface, there is a natural identification $\mathbb{Z} \equiv H^2(S;\mathbb{Z})$ and the Euler class is interpreted as an Euler number $e \in \mathbb{Z}$. Let us recall for further use how to compute this number.

Let $\pi : M \to S$ be an oriented $\mathbb{S}^1$-bundle over a closed oriented surface S of genus g. Let us consider a *small* closed disk $D \subseteq S$ and consider the surface with boundary $\check{S} := \overline{S \setminus D}$. Because of the Euler class classification, any oriented $\mathbb{S}^1$-bundle over an oriented surface with boundary is homeomorphic to a product. Furthermore, we know that the restrictions of π over D and $\check{S}$ are product bundles. Let μ_1 be the boundary of a meridian disk of the solid torus $\pi^{-1}(D)$ (oriented as ∂D), s_1 be the boundary of a section defined over $\check{S}$ (oriented as $\partial \check{S}$) and ϕ_1 be an oriented fiber in $\pi^{-1}(\partial D)$. All of these are simple closed curves that define elements in $H_1(\pi^{-1}(\partial D);\mathbb{Z})$. The fact that μ_1 and s_1 project onto generators of $H_1(\partial D;\mathbb{Z})$ implies that these elements satisfy a relation (using multiplicative notation for $H_1(\pi^{-1}(\partial D);\mathbb{Z})$)

$$s_1 \cdot \mu_1 \cdot \phi^e = 1 \tag{1.1}$$

for some $e \in \mathbb{Z}$, which happens to be the Euler number of the fibration.

There are several variations of this construction. In the first one, we can replace D and $\check{S}$ by two surfaces S_1 and S_2 with common connected boundary in such a way that $S = S_1 \cup S_2$ and formula (1.1) still holds. Moreover, there is no need to assume that the their boundaries are connected. Let us suppose that $\partial S_1 = \partial S_2 = S_1 \cap S_2$ has r connected components $C_1, \ldots, C_r$; and fix sections $s_i : S_i \to M$, $i = 1, 2$, denoting by s_i^j the boundary component of s_i projected into C_j (oriented as ∂S_i). Then, in $H_1(C_j;\mathbb{Z})$, we have inequalities

$$s_1^j \cdot s_2^j \cdot \phi^{e_j} = 1, \quad e_j \in \mathbb{Z}, \tag{1.2}$$

with $e = e_1 + \cdots + e_r$.

Moreover, any decomposition of e as above can be realized in this way in any given oriented $\mathbb{S}^1$-bundle with Euler number e.

Let us now introduce the concept of plumbing graph. A plumbing graph (Γ, g, e, o) is given by a (connected) graph Γ (without loops), a *genus function* $g : V(\Gamma) \to \mathbb{Z}_{\geq 0}$ (where $V(\Gamma)$ is the set of vertices of Γ), an *Euler function* $e : V(\Gamma) \to \mathbb{Z}$ and an *orientation* class $o \in H^1(\Gamma;\mathbb{Z}/2)$. We usually represent this graph by decorating each vertex v with $[g(v)]$ and $e(v)$, and each edge η with a sign $\sigma_\eta = \pm$ corresponding to the coefficients of a cocycle (cochain) representing o. The omission of the decoration $[g(v)]$ of a vertex means that $g(v) = 0$, and the omission of the decoration of an edge means that $\sigma_\eta = +$.

Remark 1.3 If we change a cocycle by reversing the signs of all the edges adjacent to a fixed vertex, we obtain another representative of o; moreover, we can pass from one representative to another by a sequence of these moves. Of course, if Γ is a tree, the o-decoration can be chosen to be void.

Every plumbing graph (Γ, g, e, o) has a graph manifold associated to it, given by the following construction. First, to each vertex $v \in V(\Gamma)$, we associate an oriented $\mathbb{S}^1$-bundle $\pi_v : M_v \to S_v$, over a closed oriented surface of genus $g(v)$, with Euler number $e(v)$. Then, for each edge η with endpoints v, w, we collect two closed disks $D_v^\eta \subset S_v$ and $D_w^\eta \subset S_w$. We choose these disks in such a way that they are pairwise disjoint for any fixed v. We continue by defining $\check{M}_v$ as the closure of $M_v \setminus \bigcup_{v\in\eta} \pi_v^{-1}(D_v^\eta)$, which is an oriented manifold whose boundary is composed by tori, as many as the valency of v in Γ. Then, we define $T_v^\eta := \pi_v^{-1}(\partial D_v^\eta)$. In each of these tori, we have a pair of curves $(\phi_v^\eta, \mu_v^\eta)$, where ϕ_v^η is an oriented fiber and μ_v^η is a meridian of the solid torus $\pi_v^{-1}(D_v^\eta)$ (oriented as ∂D_v^η). Notice that these curves provide a basis of $H_1(T_v^\eta; \mathbb{Z})$ consistent with the orientation of T_v^η induced by $\check{M}_v$.

Let us consider a homeomorphism $\Phi_{v,w}^\eta : T_v^\eta \to T_w^\eta$ such that $\Phi_{v,w}^\eta(\phi_v^\eta) = (\mu_w^\eta)^{\sigma_\eta}$ and $\Phi_{v,w}^\eta(\mu_v^\eta) = (\phi_w^\eta)^{\sigma_\eta}$. That is, an homeomorphism interchanging sections and fibers, according to the sign of the vertex. This map is determined up to isotopy by the matrix $\sigma_\eta \left(\begin{smallmatrix} 0 & 1 \\ 1 & 0 \end{smallmatrix}\right)$ of determinant -1. In fact, these maps are well defined only up to isotopy, and we can choose representatives such that $\Phi_{w,v}^\eta = (\Phi_{v,w}^\eta)^{-1}$.

The plumbing manifold associated to (Γ, g, e, o) is defined as:

$$\left(\coprod_{v\in V(\Gamma)} \check{M}_v \right) \Big/ \{\Phi_{v,w}^\eta\}_\eta$$

which is clearly a graph manifold. We will drop any reference to o if it is trivial.

Remark 1.4 Notice that the former construction depends on a fixed choice of a cocycle. Let us fix a vertex v and consider the cocycle $\tilde{\sigma}$ given by

$$\tilde{\sigma}_\eta = \begin{cases} \sigma_\eta & \text{if } v \notin \eta \\ -\sigma_\eta & \text{if } v \in \eta \end{cases}$$

The construction associated to $\tilde{\sigma}$ yields the same fibrations for $w \neq v$. However, for v, we obtain the fibration $\tilde{\pi}_v : M_v \to (-S_v)$, which is the opposite fibration to π_v, but the orientation of M_v remains unchanged. This implies that $\tilde{\phi}_v^\eta = (\phi_v^\eta)^{-1}$ and $\tilde{\mu}_v^\eta = (\mu_v^\eta)^{-1}$ for $v \in \eta$. Therefore, $\tilde{\Phi}_{v,w}^\eta = \Phi_{v,w}^\eta$, and the resulting manifold is the same. Hence, by Remark 1.3, the manifold depends only on o and not on the particular choice of a representative cocycle.

Example 1.5 Let X be a complex surface and $D = \bigcup_{j=1}^r D_j$ a normal crossing compact divisor in X. Let Γ be the dual graph of D and define the functions g and e as the genus and self-intersection. Then the boundary of a regular neighborhood of D is homeomorphic to the graph manifold of (Γ, g, e, o), where o is the null class. If the intersection matrix of D is negative definite, then D can be obtained as the exceptional divisor of a resolution of an isolated surface singularity. That is, the link of an isolated surface singularity is always a plumbing manifold, whose graph is the dual graph of the resolution.

2 Description of the method

In this section, we describe the method for constructing a Heegaard splitting of a graph manifold, that is the goal of this work. The method starts with a plumbing graph and, from it, through a series of steps, a Heegaard diagram is constructed.

Theorem 2.1 *Let M be a manifold associated to a plumbing graph (Γ, g, e, o). Fix a cocycle representing o (described as a choice of a sign for each edge) and a spanning tree $\mathcal{T}$ of Γ. Then, the method described in* (G1)–(G7) *provides an explicit Heegaard diagram of M.*

Fig. 1 Example graph

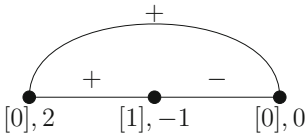

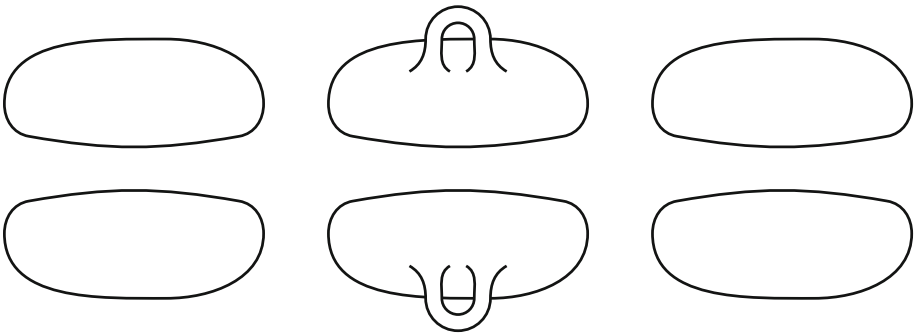

Fig. 2 Top and bottom vertex surfaces of (G1)

The rest of the section describes the steps of the method. For the sake of clarity, they are exemplified for the graph manifold of Fig. 1, where $\mathcal{T}$ is formed by the two straight edges. The proof will be developed through the rest of the paper. We will break up the proof in several cases in order to help the reader and isolate the technical difficulties for each case.

From Γ, we will construct a surface with two systems of curves, referred to as the system of *blue* curves and the system of *red* curves; these curves are the cutting curves of a Heegaard diagram of M. The steps of the process are the following:

(G1) For each vertex v, we consider a pair of closed oriented surfaces of genus g_v, called *top* and *bottom*, as in Fig. 2 for our example.

(G2) On each pair, we join the two surfaces by a number of cylinders. To each of these cylinders, we assign a plus or minus sign, satisfying the condition that, on each pair, the sum of the signs of the cylinders matches the number e_v of the corresponding vertex. The number of these cylinders can be chosen freely, as long as the previous condition holds, and there are enough of them to perform the rest of the steps in the algorithm. Besides, on each pair of surfaces, one of the cylinders is chosen as a *main cylinder*. Figure 3 shows this step performed in our example. The main cylinders are drawn thicker.

(G3) Let us consider a vertex, and then choose one surface from the corresponding pair. For each handle in this surface (if there is any), we add a red curve that turns around the handle meridian, passes through the main cylinder all the way to the other surface of the pair, follows the same path in the other surface (reversing direction) and returns back to the starting point traversing again the main cylinder (without self-intersections). Another red curve is constructed in the same way but following the handle longitude instead of the meridian. We repeat this procedure on each pair. The step is shown in Fig. 4 for the genus one vertex of our example.

(G4) For each cylinder C that is not a main cylinder, we add a red curve that goes through the main cylinder and returns through C, as shown in Fig. 5 of our example.

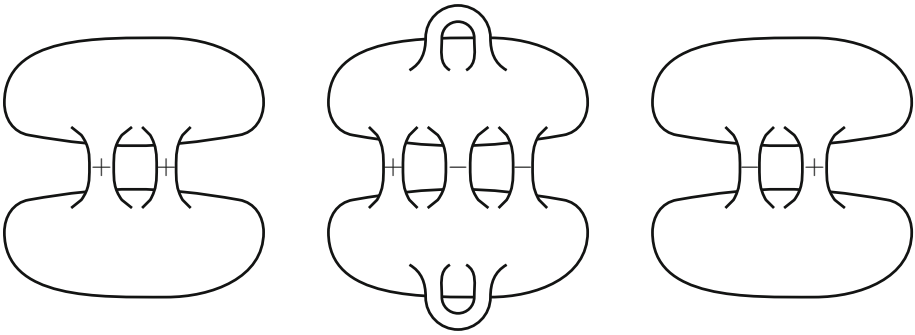

Fig. 3 Connexion by cylinders of (G2)

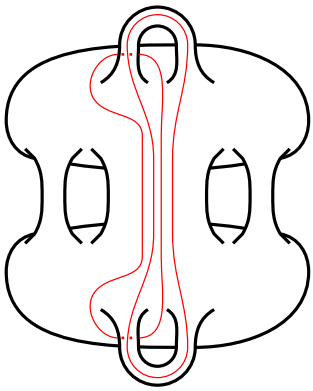

Fig. 4 Handle red curves of step (G3) for the surfaces of the genus 1 vertex

(G5) For each red curve, we add a blue curve. These blue curves should be parallel to the red curves, except for performing a Dehn twist around each cylinder they cross. The direction of the Dehn twist is given by the sign of the cylinder. This step is shown in Fig. 6 for our example.

(G6) At this point, we have constructed a surface corresponding to each vertex. We proceed now to connect these surfaces as the edges of the tree $\mathcal{T}$ would indicate. Let us choose an edge from $\mathcal{T}$ and consider the two surfaces corresponding to the vertices connected by the edge. Let s be the sign of the edge; then, we choose a cylinder with sign s in each of the surfaces. These cylinders should be crossed only by one line of each color (i.e., distinct from the main one when the corresponding surface has either more than two cylinders or positive genus). Then we cut each of these two cylinders by the middle, obtaining four boundary components or stumps. Then we glue the two upper stumps, connecting the two upper surfaces, and the two lower stumps, connecting the two lower surfaces. The red lines are just directly glued. The blue lines are also glued in such a way that new blue curve goes parallel to the new red curve in one of the new cylinders, but performs a Dehn twist around the other one. The direction of the Dehn twist is given by the sign s of the edge. Then, we repeat for each of the edges of $\mathcal{T}$. This step is shown in Figs. 7 and 8 for our example.

(G7) For the edges not in $\mathcal{T}$, we proceed similarly as before. For each of these edges, we perform (G6) just as before. However, we add yet another red curve and blue curve, constructed as follows. Let us call δ_r and γ_r the two red curves we had before performing

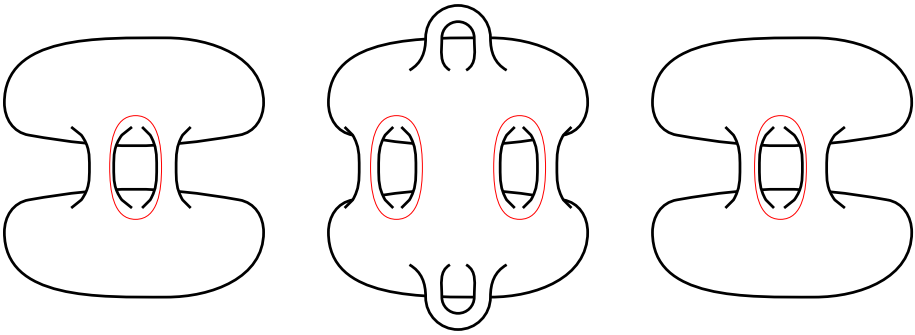

Fig. 5 Red curves in step (G4)

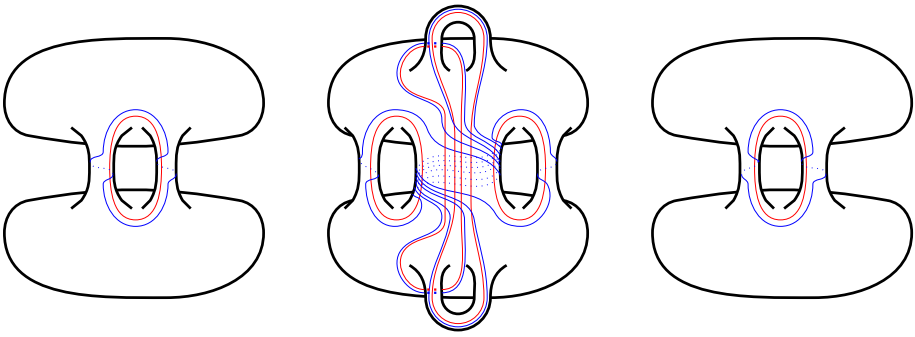

Fig. 6 All lines added after step (G5)

(G6). Let us choose (arbitrarily) one of these, say γ_r. This curve can be decomposed as $\gamma_1 \cdot \gamma_2$, where γ_2 is the path contained in the cylinder that is going to be cut. Then, after performing (G6), we take two parallel copies of γ_1 and connect them by surrounding the newly formed cylinders, in such a way that the resulting curve is disjoint with the red curve created by performing (g6). This is going to be the extra red curve. Then, another blue curve is created in exactly the same way. As before, let δ_b be one of the original blue curves. Then δ_b can be decomposed as $\delta_1 \cdot \delta_2$, where δ_2 is the path contained in the cylinder to be cut. After performing (G6), we take two parallel copies of δ_1 and connect them by surrounding the newly formed cylinders, in such a way that the resulting curve is disjoint with the blue curve created by performing (G6). We take this as the extra blue curve. This step is shown in Fig. 9 for our example.

3 Topological constructions

In this section, we introduce different constructions which will be used in the sequel.

Definition 3.1 A (g, n)-*drilled body* is a product $H_{g,n} := \Sigma_{g,n} \times I$, where $I := [0, 1]$ and $\Sigma_{g,n}$ is an oriented compact surface of genus g and n boundary components, with $n > 0$ (Fig. 10b, c).

Theorem 3.2 *A* (g, n)*-drilled body is a* $(2g + n - 1)$*-handlebody.*

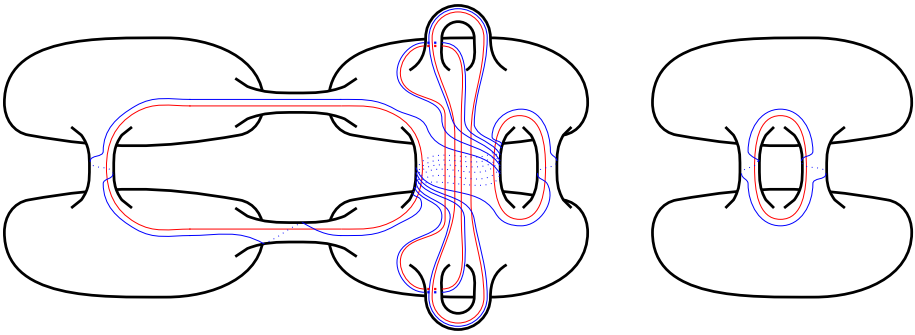

Fig. 7 Curves after adding one edge in step (G6)

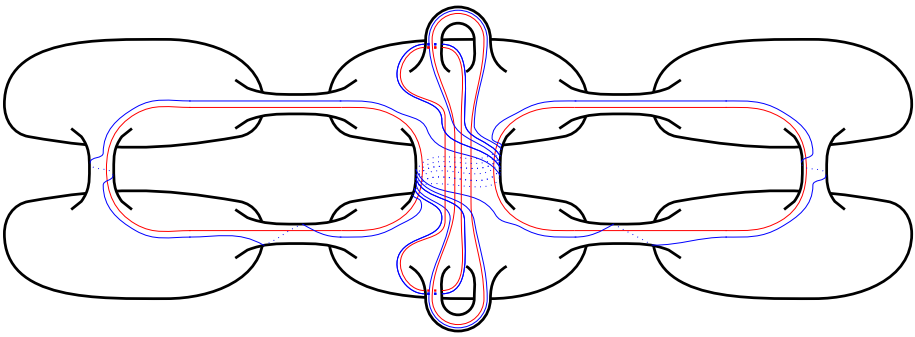

Fig. 8 Curves after adding the second edge in step (G6)

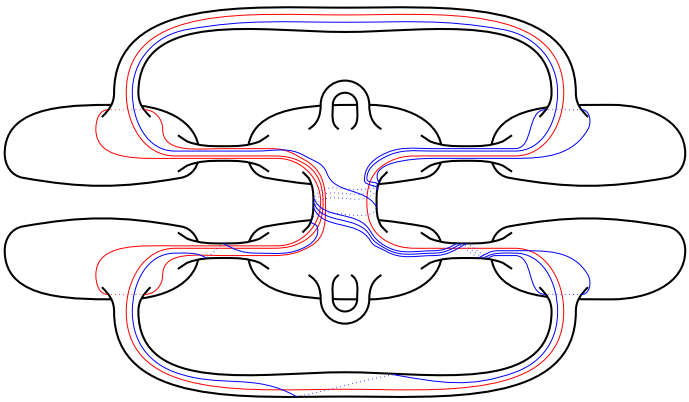

Fig. 9 Curves after step (G7). The Handle curves have been omitted for clarity

Proof This is clear if we see the base space as a fundamental polygon with subtracted disks in Seifert's fashion. □

The boundary of a (g, n)-drilled body is therefore an oriented surface of genus $2g + n - 1$ which can be decomposed as a union of two copies of $\Sigma_{g,n}$ and n cylinders, that we call *drill holes*.

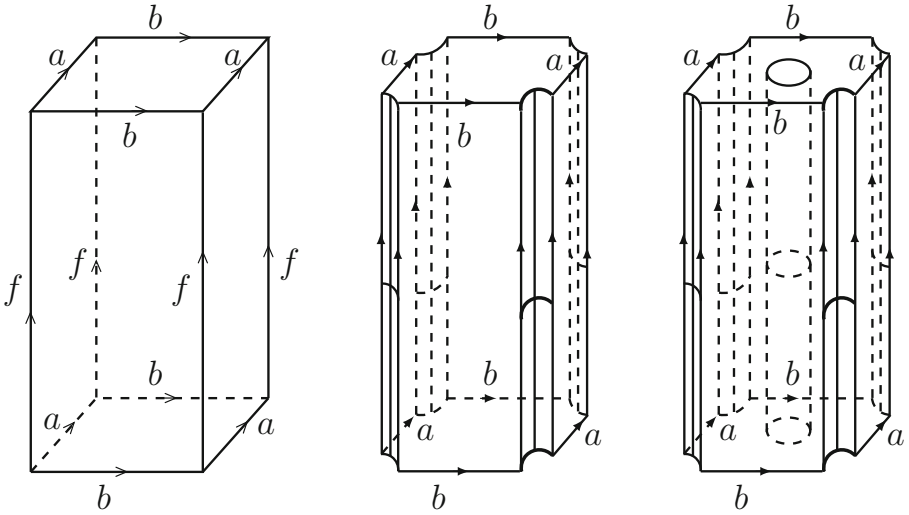

Fig. 10 Products. **a** $(\mathbb{S}^1)^2 \times I = \Sigma_{1,0} \times I$, **b** $H_{1,1}$, **c** $H_{1,2}$

We introduce now another construction. Let M be an oriented 3-manifold with boundary, and let η be an oriented simple closed curve in ∂M. Then a regular neighborhood C of η in ∂M is an annulus. Let V be an oriented solid torus, γ a longitude in ∂V, and A a regular neighborhood of γ in ∂V, which is again an annulus. Finally, let $\psi : C \to A$ be an orientation-reversing homeomorphism. The following proposition is clear.

Proposition 3.3 *The manifold $M \cup_\psi V$ is homeomorphic to M.*

Remark 3.4 Notice that in the previous construction there are two possible choices for the gluing morphism ψ. One of them identifies γ with η and the other with η^{-1}. Moreover, the gluings of the boundary components of C and A are interchanged.

Definition 3.5 The above operation is called a *float gluing* of M along C.

Definition 3.6 Given a handlebody M of genus g, we say that a simple closed curve $\gamma \subset \partial M$ is a *float curve* if there is a cutting system of curves in ∂M (i.e., boundaries of meridian disks, such that M cut along the disks is a ball) satisfying that γ intersects this system in only one point, and this intersection is transverse.

Example 3.7 Let V_1 be a solid torus with a longitude γ. Let V_{g-1} be a handlebody of genus $g-1$. By gluing two disks in the boundaries of V_1 and V_{g-1}; we obtain a new handlebody V_g. For further use, we will refer to this operation as the *handle sum* of V_1 and V_{g-1}. We can assume that γ is disjoint from the disk in ∂V_1 used for the handle sum. Then $\gamma \subset V_g$ is a *float curve* of V_g, since it only cuts the meridian of V_1.

Definition 3.8 The pair (V_g, γ) is called a *standard float-curve system* of genus g.

The following lemma is clear.

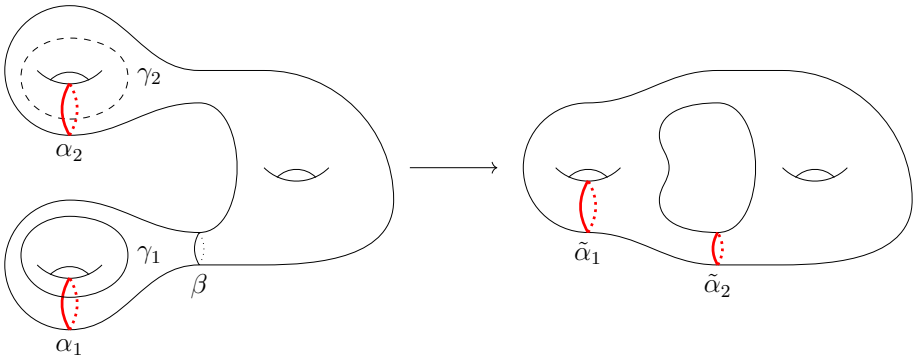

Fig. 11 Gluing disjoint float curves in a handlebody

Lemma 3.9 *Let M be a handlebody of genus g and let $\gamma \subset M$ be a float curve. Then, the pair (M, γ) is homeomorphic to a standard float-curve system of genus g.*

Proposition 3.10 *Let M_1, M_2 be two handlebodies of genus $g_1, g_2 \geq 1$. Let us fix float curves γ_1 and γ_2 in each of these, and consider regular neighborhoods A_1 and A_2 of these curves in ∂M_1 and ∂M_2, respectively. Let $\psi : A_1 \to A_2$ be an orientation-reversing homeomorphism. Then, $M_1 \cup_\psi M_2$ is a handlebody of genus $g_1 + g_2 - 1$.*

Remark 3.11 If M_2 is a torus, the above operation is a particular case of float gluing since we only need the curve in the solid torus to be a float curve. In fact, the above proposition remains true if we only ask γ_2 to be a float curve, but we do not use this more general fact.

Proof Notice that M_2 can be constructed as a handle sum of a solid torus V_1 and a handlebody of genus $g_2 - 1$. This operation can be performed in such a way that $A_2 \subset V_1$ and γ_2 is a longitude of V_1.

Then, the gluing of M_1 and M_2 can be performed as a float gluing followed by a handle sum. □

A similar idea can be used for the identification of two different annuli in a single handlebody.

Proposition 3.12 *Let M be a handlebody of genus $g \geq 2$. Let us fix a cutting system of curves and two disjoint float curves γ_1 and γ_2 intersecting different curves α_1 and α_2 of a cutting system . Let A_1 and A_2 be regular neighborhoods of γ_1 and γ_2, respectively, and let $\psi : A_1 \to A_2$ be an orientation-reversing homeomorphism. Then the quotient M_ψ of M by ψ is a handlebody of genus g.*

Proof Up to homeomorphism, we may assume that the float curves are standard ones. The manifold M can be seen as the handle sum of two handlebodies M_1 and M_2, of genera 1 and $g - 1$, and containing A_1 and A_2, respectively. It is equally clear that γ_1 and γ_2 are float curves in each of these handlebodies. By Proposition 3.10, $M_1 \cup_\psi M_2$ is a handlebody of genus $g - 1$. By performing the handle sum that joins M_1 and M_2 into M, one more handle is created. □

Remark 3.13 In Fig. 11, it can be seen how a new cutting curve is obtained by joining the two identified ones, and another one appears for the handle corresponding to the handle sum; it is easily seen that the latter is the commutator of α_1 and γ_1.

4 Heegaard splitting of $\mathbb{S}^1$-bundles over surfaces with unimodular Euler number

The goal of this section is to prove Theorem 2.1 when M is an $\mathbb{S}^1$-bundle over a surface of genus g with Euler number ± 1. This is the case where the graph Γ has only one vertex, decorated with $([g], \pm 1)$, and no edges.

Let $\pi : M \to S$ be an oriented $\mathbb{S}^1$-bundle over a closed oriented surface S of genus g, with Euler number $e = \pm 1 \in \mathbb{Z} \equiv H^2(S; \mathbb{Z})$. Let us consider a small closed disk $D \subseteq S$ and the surface with boundary $\check{S} := \overline{S \backslash D}$. Since $H^2(\check{S}; \mathbb{Z})$ is trivial, there exists a section $s_1 : \check{S} \to M$ of π. We take this section and another *parallel* section s_2. These two sections divide $\check{M} = \pi^{-1}(\check{S})$ in two pieces M_1 and M_2; which are oriented compact 3-manifolds with boundary, and satisfy that $M_1 \cap M_2 = \partial M_1 \cap \partial M_2 = \mathbf{S} \coprod \mathbf{N}$, where $\mathbf{S} := s_1(\check{S})$ and $\mathbf{N} := s_2(\check{S})$.

Convention 4.1 Once the two sections s_1, s_2 have been chosen, we choose M_1 and M_2 in such a way that the orientations on $\mathbf{N}$ induced by M_1 and s_2 coincide. This means that a positive half-fiber inside M_1 goes from $\mathbf{S}$ to $\mathbf{N}$.

The boundary of M_1 is obtained by gluing $\mathbf{S}$ and $\mathbf{N}$ with an annulus C which fibers over $\partial D = \partial \check{S}$ (whose fibers are positive half-fibers inside M_1 homeomorphic to $[0, 1]$). In the same way $\partial M_2 = \mathbf{S} \cup C' \cup \mathbf{N}$, where C' is the other annulus in M_2. Notice that $C \cup C'$ is the torus $\pi^{-1}(\partial D) = \partial \pi^{-1}(D)$ and C and C' have common boundaries.

Proposition 4.2 *The 3-manifolds M_1, M_2 are $2g$-handlebodies.*

Proof The manifold M_1 is, by construction, the drilled body $H_{g,1}$, see Theorem 3.2. Since M_2 is homeomorphic to M_1, it is also a $2g$-handlebody. □

Theorem 4.3 *Let $\tilde{M}_2 := M_2 \cup \pi^{-1}(D)$. Then the manifold $\tilde{M}_2$ is homeomorphic to M_2 and, hence, it is a $2g$-handlebody ($e = \pm 1$ is an essential hypothesis).*

Proof Notice that C' is the annulus along which M_2 and $\pi^{-1}(D)$ are glued. Let K be the core of this annulus. Since $e = \pm 1$, K is homologous to the core of $\pi^{-1}(D)$ and the statement follows from Proposition 3.3. □

Corollary 4.4 *The submanifolds M_1 and $\tilde{M}_2$ form a Heegaard splitting of M of genus $2g$.*

Proposition 4.5 *Let M be the graph manifold obtained as an $\mathbb{S}^1$-bundle over a surface of genus g and Euler class ± 1. Then, the statement of Theorem 2.1 holds for M.*

Let us summarize the steps in Sect. 2 that are to be applied in this case. The process starts with (G1), followed by (G2), where only the main cylinder is needed. The last steps are (G3) and (G5). The resulting diagram can be depicted as in Fig. 13b.

Proof It is clear that the surface $\Sigma_1 := \partial M_1 = \partial \tilde{M}_2$ (oriented as boundary of M_1), which is the gluing of $\mathbf{S}$, $\mathbf{N}$ and the cylinder $C \cong \partial D \times I$, is the surface constructed in (G2). Notice that $\mathbf{N}$ inherits the orientation of S while $\mathbf{S}$ inherits the opposite one.

Let us prove that the red curves constructed in (G3) form a system of cutting curves for M_1.

To construct a system of cutting curves for M_1 in Σ_1, we see M_1 as a prism as in Fig. 10b. Then, its system of cutting curves is formed by two families of curves:

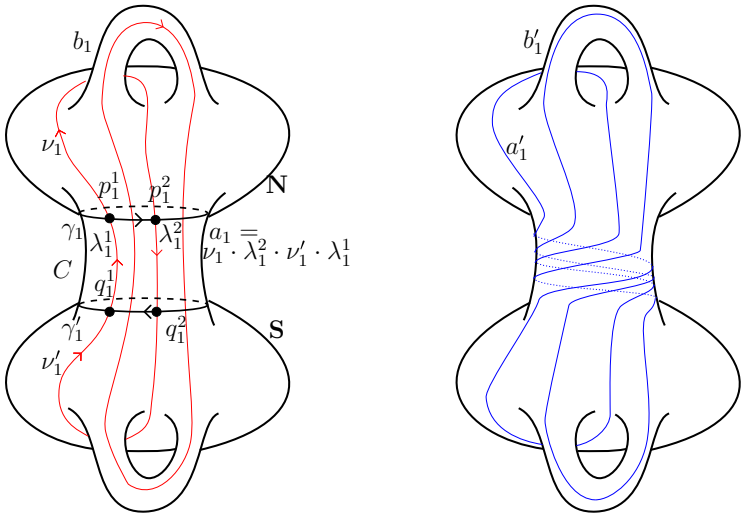

Fig. 12 **a** Cutting curves for M_1. **b** Cutting curves for $\tilde{M}_2$, $e = 1$

- From half of the identified faces in the prism (Fig. 10b), we obtain curves $a_1, \ldots, a_g$, that can be described as composed by four paths as follows (see Fig. 12a). Consider points p_i^1, p_i^2 in $C \cap \mathbf{N}$ and points q_i^1, q_i^2 in $C \cap \mathbf{S}$ such that there are half-fibers λ_i^1 (from q_i^1 to p_i^1) and λ_i^2 (from p_i^2 to q_i^2). Pick up a path ν_i in $\mathbf{S}$ from p_i^1 to p_i^2 which turns around the ith handle like its meridian. We construct a path ν_i' in $\mathbf{N}$ in a similar way with reversed orientation. Then, $a_i := \nu_i \cdot \lambda_i^2 \cdot \nu_i' \cdot \lambda_i^1$. It is possible to choose these cycles to be pairwise disjoint.
- Similarly, from the other half of the identified faces, we obtain curves $b_1, \ldots, b_g$. These are constructed in the same way as the a_i's, but instead of taking ν_i and ν'_i, we take paths that turn around the handles like their longitudes. These paths are chosen in such a way that they do not intersect each other and they are also disjoint to the paths a_i's.

These are exactly the red curves constructed in (G3). The next step is the construction of the blue curves from (G5), i.e., the system of cutting curves for $\tilde{M}_2$.

We start with M_2 (homeomorphic copy of M_1) which is constructed in the same way as M_1 but using the other cylinder C'. Recall that the union of the two cylinders C and C' along their common boundary yields the torus $\mathbb{T} := \pi^{-1}(\partial D)$, the boundary of the solid torus $\pi^{-1}(D)$. So the construction of the system of cutting curves for M_2 will mimic the one for M_1 replacing the cylinder C by C'.

Since $\tilde{M}_2 = M_2 \cup \pi^{-1}(D)$, let us consider the situation at $\pi^{-1}(D)$. In order to fix the orientations, we assume that $e = 1$, leaving the case $e = -1$ for later. The solid torus $\pi^{-1}(D)$ is represented as a cylinder whose bottom and top are glued by a vertical translation in Fig. 13a.

In the torus $\mathbb{T}$, we fix the product structure with an oriented section μ_1 (the boundary of a disk in the solid torus) and an oriented fiber ϕ_1. Let us fix one cutting curve (a_i or b_i) of M_1; it intersects the cylinder C in two half-fibers. Let λ_1 be the one from $\mathbf{S}$ to $\mathbf{N}$; let λ_2 be the other half of the fiber in C' (which is part of a cutting curve in M_2) but with opposite orientation, in order to go again from $\mathbf{S}$ to $\mathbf{N}$; i.e., $\lambda_1 \cdot {\lambda_2}^{-1}$ is homologous to ϕ_1 in $\mathbb{T}$.

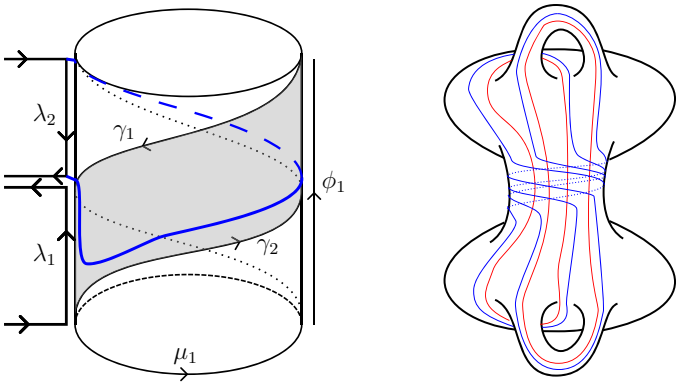

Fig. 13 **a** From M_2 to $\tilde{M}_2$, $e = 1$. **b** Example for the case $g = 1$, $e = -1$

The cylinders C and C' have as common boundaries two cycles $\gamma_1 \subset \mathbf{N}$ and $\gamma_2 \subset \mathbf{S}$, oriented as boundaries of these surfaces; in Fig. 13a, the front part of C is colored. The homology class of γ_1 in $\mathbb{T}$ is (with multiplicative notation) $\mu_1^{-1} \cdot \phi_1^{-e}$ (recall $e = 1$ in Fig. 13a), since the definition of Euler number implies that $\gamma_1 \cdot \mu_1 \cdot \phi_1^e$ is trivial.

The cycle $(\gamma_2)^{-1} \cdot (\lambda_1 \cdot {\lambda'_1}^{-1})^e \sim \gamma_1 \cdot \phi_1^e \sim \mu_1^{-1}$ bounds a disk in $\pi^{-1}(D)$. The union of this disk with the cutting disk of M_2 containing ${\lambda_2}^{-1}$ in its boundary provides a new disk where ${\lambda'_1}^{-1}$ is no more in its boundary. If we repeat this process with the other half-fiber in the cutting curve, we obtain the corresponding cutting curve in $\tilde{M}_2$ where the half-fibers have been replaced by curves in $C \subset \partial \tilde{M}_2 = \partial M_1$. It can be checked that the retraction seen in Proposition 3.3 sends $\gamma_2^{-e}\lambda_1$ to λ_2 and hence this construction provides the cutting curve for $\tilde{M}_2$.

Figure 12b shows the cutting curves of $\tilde{M}_2$ for $g = 1$, $e = 1$. Notice that the blue curves in C turn around as γ_1 when going from $\mathbf{S}$ to $\mathbf{N}$. The closed curve γ'_1 is oriented as boundary of N and γ_1 is parallel to γ'_1.

It is clear that in the case of $e = -1$, the same thing will happen but instead of turning as γ_1, the curves will turn as γ_1^{-1}, see Fig. 13b. □

5 Heegaard splitting of arbitrary $\mathbb{S}^1$-bundles over surfaces

In this section, we continue the Proof of Theorem 2.1 when M is an $\mathbb{S}^1$-bundle over a surface of genus g with arbitrary Euler number, i.e., where the graph Γ has only one vertex, decorated with $([g], e)$, and no edges.

In order to construct a Heegaard splitting for arbitrary Euler number e, we proceed as follows. Let now $\check{S} := \overline{S \setminus \bigcup_{j=1}^n D_i}$, where $D_1, \ldots, D_n$ are pairwise disjoint closed disks in S. As before, let $s_1, s_2 : \check{S} \to M$ be arbitrary parallel sections of π. For each $j = 1, \ldots, n$, let $\gamma_j := s_1(\partial D_j)$ (oriented as part of $\partial \check{S}$) and let μ_j be the boundary of a meridian disk of the solid torus $\pi^{-1}(D_j)$. By the choice of orientations, the cycle $\gamma_j \cdot \mu_j \cdot \phi^{e_j}$ is trivial in $H_1(\pi^{-1}(\partial D_j); \mathbb{Z})$, for some $e_j \in \mathbb{Z}$, where ϕ is an oriented fiber of π; these values are related with e as in (1.2).

As we did in Sect. 4, we may decompose $\check{M} := \pi^{-1}(\check{S})$ in two pieces M_1 and M_2; M_1 and M_2 are oriented compact 3-manifolds with boundary and $M_1 \cap M_2 = \partial M_1 \cap \partial M_2 = s_1(\check{S}) \coprod s_2(\check{S})$ with the same orientation convention. From Theorem 3.2, the manifolds M_1 and M_2 are $(2g + n - 1)$-handlebodies.

Let us assume that $e_j = \pm 1$, $j = 1, \ldots, n$. Notice that M_2 is homeomorphic to M_1 and hence, it is also a $(2g + n - 1)$-handlebody. Let $\tilde{M}_2 := M_2 \cup \bigcup_{j=1}^{n} \pi^{-1}(D_j)$. Following the arguments in the Proof of Theorem 4.3, we can see that $M_2 \cong \tilde{M}_2$ and M_1 and $\tilde{M}_2$ have the same boundary. We have proven the following result.

Proposition 5.1 *The submanifolds M_1 and $\tilde{M}_2$ form a Heegaard splitting of M. If $e = 0$, a decomposition of this kind of genus $2g + 1$ can be always obtained; and if $e \neq 0$, one of genus $2g + |e| - 1$.*

Remark 5.2 In this process, we have glued all the solid tori $\pi^{-1}(D_j)$ to M_2. This is not essential for the proof: we could have glued some of them to M_1 and the result would be equally valid.

Proposition 5.3 *Let M be the graph manifold obtained as an $\mathbb{S}^1$-bundle over a surface of genus g and arbitrary Euler class. Then, the statement of Theorem 2.1 holds for M.*

The most relevant difference with the Proof of Proposition 4.5 is that for (G2), we need extra cylinders besides the main one. Meaningful examples are shown in Fig. 14. The main technical difficulties of this proof are addressed in the Proof of Proposition 4.5.

Proof The step (G2) is involved in this proof since in order to obtain the Heegaard splitting of Proposition 5.1, we need to connect the top and bottom surfaces of (G1) with more than one cylinder.

Let us decompose the system of cutting curves of M_1, i.e., the red curves of (G3) and (G4) in two subsets. The first one (the curves in (G4)) is the system of cutting curves of M_1 in the Proof of Proposition 4.5 (passing through the *main cylinder* $\partial D_1 \times I$).

For the second one, the red curves in (G4), we start with suitable paths α_j $(j = 2, \ldots, n)$ joining $p_j \in \partial D_1$ and $q_j \in \partial D_j$ (see Fig. 10c), such that if we cut $\check{S}$ along a_i, b_i $(i = 1, \ldots, n)$ and α_j, then a disk is obtained. The second subset is formed by the boundaries

$$c_j = s_1(\alpha_j) \cdot (\{q_j\} \times I) \cdot s_1(\alpha_j)^{-1} \cdot (\{p_j\} \times I)^{-1}.$$

of $\alpha_j \times I$; they cross the main cylinder and the corresponding $\partial D_j \times I$.

Let us describe now the blue curves of (G5). We follow the arguments in the Proof of Proposition 4.5, the curves of $\tilde{M}_2$ go parallel to the ones of M_1 except for the modification in the cylinders $\partial D_i \times I$, $1 \leq i \leq n$, due to the float gluing of the solid tori $\pi^{-1}(D_i)$. By the same reasoning as before, these modifications consist on a Dehn twist along each cylinder. The orientation of each Dehn twist depends on the sign of each e_i. □

Example 5.4 Figure 14a shows this construction for the case of genus zero and Euler number equal to 3. We choose three solid tori and sections with $e_i = 1$. The resulting Heegaard decomposition has genus 2 and therefore is not minimal, since the manifold in question is a lens space, and as such admits a genus one decomposition. Figure 14b shows an example of this construction for the case of $g = 1$, $e = 2$.

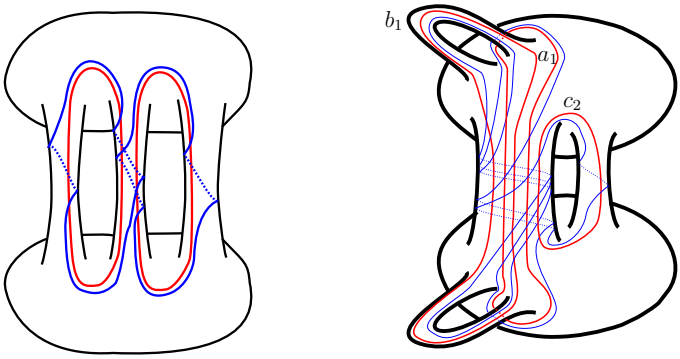

Fig. 14 **a** Example for the case $g = 0$, $e = 3$. **b** Example for the case $g = 1$, $e = 2$

6 Heegaard splitting of a plumbed graph manifold with an edge

In this section, we deal with the case when M comes from a graph with an edge and two vertices.

This manifold is obtained as follows. We start with two manifolds W_1 and W_2, which are the total space of oriented $\mathbb{S}^1$-bundles π_i over closed surfaces S_i of genus g_i and Euler numbers e_i, $i = 1, 2$. Then we take closed disks $D_{i,0} \subset S_i$ and choose a system of curves μ_i, ϕ_i on $\pi_i^{-1}(\partial D_{i,0})$ where the curve ϕ_i is an oriented fiber of π_i, and μ_i is the oriented boundary of a meridian disk of $\pi_i^{-1}(\partial D_{i,0})$.

Then, M is obtained by gluing $\pi_1^{-1}(\overline{S_1 \setminus D_{1,0}})$ and $\pi_2^{-1}(\overline{S_2 \setminus D_{2,0}})$ along their boundaries. These boundaries are tori $\pi_i^{-1}(\partial D_{i,0})$, $i = 1, 2$, and the gluing is determined, up to isotopy, by a matrix in $\mathrm{GL}(2; \mathbb{Z})$, once ordered integral bases in $H_1(\pi_i^{-1}(\partial E_i); \mathbb{Z})$ are chosen. Since we are using the plumbing construction, for the choice of $(\mu_{1,0}, \phi_1)$ and $(\mu_{2,0}, \phi_2)$, this matrix is $\pm \left(\begin{smallmatrix} 0 & 1 \\ 1 & 0 \end{smallmatrix}\right)$, depending on the sign of the edge as described in Sect. 1, i.e., we are *interchanging* fibers and sections.

Since the edge is contractible, the cohomology class o of Sect. 1 vanishes and can be represented by any sign, yielding to homeomorphic constructions.

Let us consider pairwise disjoint closed disks $D_{j,1}, \ldots, D_{j,n_j} \subset S_j \setminus D_{j,0}$, $j = 1, 2$. Let $\check{S}_j := \overline{S \setminus \bigcup_{i=0}^{n_j} D_{j,i}}$. We consider two parallel sections $s_{j,1}, s_{j,2} : \check{S}_j \to M_j := \pi_j^{-1}(\check{S}_j)$ of π_j as in Sect. 5.

As in Sect. 5, we denote $\gamma_{j,i} := s_1(\partial D_{j,i})$ (oriented as part of $\partial \check{S}_j$); let $\mu_{j,i}$ be the boundary of a meridian disk of $\pi^{-1}(D_{j,i})$. As in that section, we collect the integers $e_{j,i}$ appearing in the equalities (in homology of the boundary tori) $\gamma_{j,i} \cdot \mu_{j,i} \cdot \phi_j^{e_{j,i}} = 1$, where ϕ_j is a fiber of π_j, and the equality

$$\sum_{i=0}^{n_j} e_{j,i} = e_j,$$

must be satisfied due to (1.2).

In order to construct Heegaard splittings $M_1^j, \tilde{M}_2^j$ of W_j, $j = 1, 2$, as in Sect. 5 using the systems of disks $\{D_{j,0}, \ldots, D_{j,n_j}\}$, we need the condition $|e_{j,i}| = 1$. To perform the plumbing method, we need to have more than one cylinder in the construction of the Heegaard

splittings M_1^j, $\bar{M}_2^j$, i.e., $\min\{n_1, n_2\} \geq 1$. Moreover, in order to apply the step (G5), we impose that $\partial D_{j,0} \times I$ is not the main cylinder, $j = 1, 2$ and that $\varepsilon := e_{1,0} = e_{2,0}$ equals the sign of the edge.

More precisely, we have to remove $\pi_j^{-1}(\mathring{D}_{j,0})$ from $\tilde{M}_2^j$, but as we saw before, this operation does not change the topology (since it is the inverse of a float gluing). Let us denote by N_2^j the result of the removal of $\pi_j^{-1}(\mathring{D}_{j,0})$ from $\tilde{M}_2^j$.

Notice that after the plumbing, $\mu_{1,0}$ is identified with ϕ_2^ε, and $\mu_{2,0}^\varepsilon$ is identified with ϕ_1. This implies that $\gamma_{1,0}$ and $\gamma_{2,0}$ are homologous after the plumbing (because of the choice of the edge sign). In particular, it means that we can choose the sections $s_{j,i}$ in such a way that $s_{j,1}(\partial D_{1,0})$ is identified with $s_{j,2}(\partial D_{2,0})$. This way, the two Heegaard splittings are compatible, and we can extend them to a decomposition of M.

Summarizing, we have now the following decomposition:

$$M = \left(M_1^1 \cup M_1^2\right) \bigcup \left(N_2^1 \cup N_2^2\right). \tag{6.1}$$

Proposition 6.1 *The manifolds $M_1^1 \cup M_1^2$ and $N_2^1 \cup N_2^2$ are handlebodies, i.e., decomposition (6.1) is a Heegaard splitting of M.*

Proof It is enough to prove it for $M_1^1 \cup M_1^2$. We have already seen that both M_1^1 and M_1^2 are handlebodies. We will show now that they are glued as in Proposition 3.10. In order to do so, we have to see that they are glued along annuli that are neighborhoods of a float curve.

Let us consider the torus $\pi_i^{-1}(\partial D_{1,0})$ as the product of $\mu_{1,0}$ and ϕ_1. The curves $s_{1,i}(\partial D_{1,0})$ are parallel curves that meet ϕ_1 transversally at only one point. Let

$$A_1^1 = M_1^1 \cap \pi_i^{-1}(\partial D_{1,0})$$

be the annulus along which the gluing is made. This annulus is a neighborhood of a curve parallel to $s_{1,i}(\partial D_{1,0})$.

From the construction in Sect. 5, we see that $\phi_1 \cap M_1^1$ is part of a cutting curve of M_1^1. And moreover, its the only intersection of a cutting curve with the torus $\pi_i^{-1}(\partial D_{1,0})$.

So the annulus A_1^1 is a regular neighborhood of a float curve in M_1^1. Analogously, A_1^2 is also a float curve in M_1^2. By Proposition 3.10, we get the result. □

Proposition 6.2 *Let M be the graph manifold obtained from a graph with one edge and two vertices. Then, the statement of Theorem 2.1 holds for M.*

Proof We start applying steps (G1)–(G5) for each vertex. We are going to prove that the blue and red curves of (G6) (for the edge) produce the system of cutting curves for $M_1^1 \cup M_1^2$ (red) and $N_2^1 \cup N_2^2$ (blue).

Consider the cylinders $A_1^1 \subset M_1^1$ and $A_1^2 \subset M_1^2$ which are identified by the plumbing. The (red) cutting curves of M_1^1 (resp. M_1^2) disjoint with A_1^1 (resp. A_1^2) remained unchanged. Let us see how the other two curves behave (one for M_1^1 and one for M_1^2).

Let λ_1 be the cutting curve of M_1^1 which intersects once the core of A_1^1 (which is a float curve). In the neighborhood of A_1^1, this curve is decomposed in three pieces $\lambda_1^b, \lambda_1^c, \lambda_1^e$ where λ_1^c is the part of λ_1 that lies in A_1^1. As in the Proof of Proposition 4.5, the path λ_1^c is a half of the fiber ϕ_1. Analogously, the cutting curve λ_2 in M_1^2 in a neighborhood of A_1^2 can be divided in three pieces $\lambda_2^b, \lambda_2^c, \lambda_2^e$. The path λ_2^c is a half of a fiber ϕ_2, and recall that ϕ_2 is identified with a section μ_1. These decompositions are illustrated in Fig. 15a.

Let us decompose $\gamma_1 = \eta_1 \cdot \eta_2$ in two halves where η_1 is the bottom part in Fig. 15a (joining the endpoint of λ_2^c and the starting point of λ_1^c). If $e_{i,0} = 1$, we can check that λ_2^c can

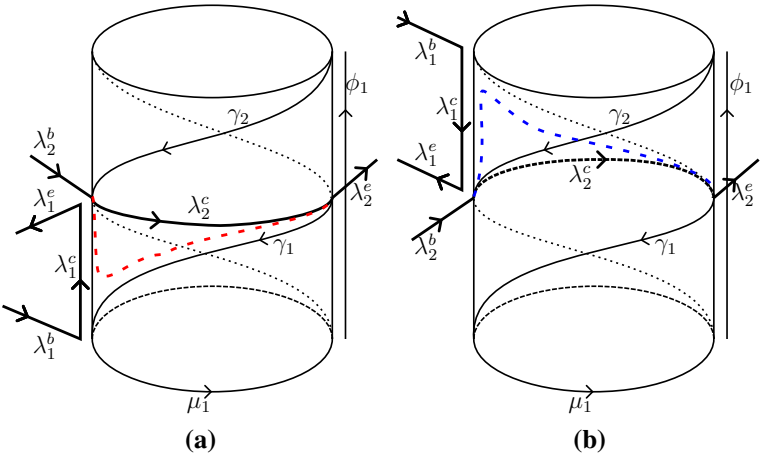

Fig. 15 **a** Gluing of M_1^i, $e_{i,0} = 1$. **b** Gluing of N_2^i, $e_{i,0} = 1$

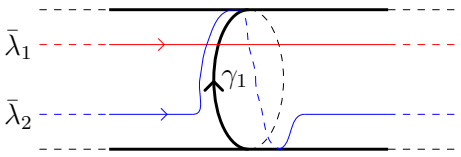

Fig. 16 Cutting curves for $e_{i,0} = 1$

be isotoped inside A_1^1 to $(\lambda_1^c)^{-1}$ followed by $(\eta_1)^{-1}$, see Fig. 15a. The new cutting curve $\bar{\lambda}_1$ is the boundary of the union of the disks bounded by λ_1 and λ_2 and the *triangle* (in $A_1^1 \equiv A_1^2$) limited by λ_1^c, λ_2^c, η_1. Notice that $\bar{\lambda}_1$ has two connected components near $A_1^1 \equiv A_1^2$; one being $\lambda_2^b \cdot \lambda_1^e$, and the other one $\lambda_1^b \cdot (\eta_1)^{-1} \cdot \lambda_2^e$.

We perform a similar argument for the gluing of N_1^2 and N_2^2. Notice that the main difference between M_j^i and N_j^i is the gluing of the extra solid tori, but the tori involved in the plumbing have been removed.

In this case, we consider the other annuli $A_2^1 \subset N_1^2$ and $A_2^2 \subset N_2^2$ that become identified; these are the other parts of the plumbing tori. Let us choose cutting curves λ_1', λ_2' that go parallel to λ_1, λ_2 near the annuli. In order to emphasize this, we keep the above notation for their decomposition in the neighborhood of the annuli, see Fig. 15b. Assuming again $e_{i,0} = 1$, we see that λ_1^c can be isotoped inside A_2^1 to λ_2^c followed by η_2; notice that the isotopy is done in the back part of A_2^1 in Fig. 15b. The new (blue) cutting curve $\bar{\lambda}_2$ has two connected components near $A_2^1 \equiv A_2^2$; one being $\lambda_2^b \cdot \lambda_1^e$, as before, and the other one $\lambda_1^b \cdot \eta_2 \cdot \lambda_2^e$.

As we see in Fig. 15a, b, some of the ends do not fit; in order for them to fit, we have to do a half-turn around γ_1 in the suitable direction. Since we have freedom to choose the product structure in the annulus, this is equivalent to keep the intersection of the red curves as fibers, while the intersection of the blue curves perform a full loop, as explained in (G6). To be precise, since the curve $\bar{\lambda}_2 \cdot (\bar{\lambda}_1)^{-1}$ equals γ_1 near the plumbing (in homology), for $e_{i,0} = 1$ the curve λ_2 turns as γ_1 (when going from the first vertex to the second one), see Fig. 16. It is easily seen that it turns as γ_1^{-1} for $e_{i,0} = -1$. □

Example 6.3 Figure 17 illustrates the case of two vertices with genus zero and both with Euler number -2. Notice that we take $n_1 = n_2 = 1$ and $e_{i,j} = -1$.

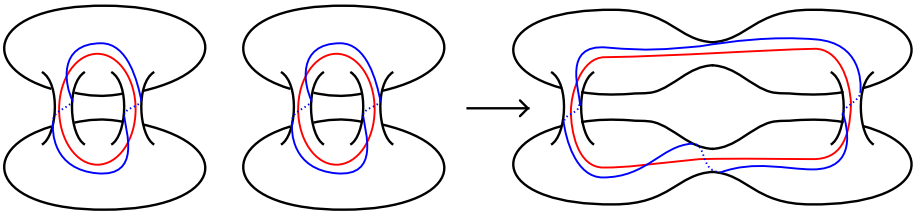

Fig. 17 Heegaard diagram of the plumbing of two manifolds with $g = 0, e = -2$

7 Heegaard splitting of arbitrary graph manifolds

Proof of Theorem 2.1 Let (Γ, g, e, o) be an arbitrary plumbing graph. As indicated in the statement, we fix an explicit cocycle representing o, consisting on assigning a sign e_η to each edge η.

Let us fix a vertex v with valency d_v, associated to a fibration $\pi_v : M_v \to S_v$. Let us choose $d_v + n_v$ pairwise disjoint closed disks in S_v, determining solid tori in M_v. The first d_v disks are assigned to a fixed edge η having v as an endpoint. As in Sect. 6, the first d_v disks will have associated numbers e_η, and the remaining disks numbers $e_{v,j}$, $j = 1, \ldots, n_v$, such that their absolute value equals 1, and

$$\sum_{v \in \partial \eta} e_\eta + \sum_{j=1}^{n_v} e_{v,j} = e_v.$$

Since the method needs a main cylinder for each vertex, n_v must be at least one. As an exception, this condition can be relaxed when $g_v = 0, d_v = 2, e_v \in \{-2, 0, 2\}$, since in this case the main cylinder may play no special role.

If Γ is a tree, it is enough to iterate the construction of the Proof of Proposition 6.2. Notice also that there is no restriction for the choice of the cocycle.

Let us now consider the general case where the graph may have cycles. This is the only case where (G7) plays a role. We proceed as before for all the edges in the spanning tree $\mathcal{T}$. Let us now explain the effect of the plumbing process along the remaining edges.

As we saw in Proposition 3.12, the process is different when the plumbing closes a cycle in the graph. This is because the gluing process is done between two float curves of the same handlebody. In particular, the way of constructing cutting curve systems changes. Proposition 3.12 proves that this process produces also a Heegaard splitting (where the genus remains unchanged).

How to obtain the cutting curves is explained in Remark 3.13. Figure 18 describes this process in our case, showing how to obtain the new pair of cutting curves from the ones that existed before the plumbing. The first pair of cutting (red and blue) curves is obtained as in the tree case: they are obtained as connected sum of the preexistent ones. The second pair of cutting curves is constructed as explained in Remark 3.13, as the union of two parallel copies of a preexistent curve and the boundaries of the identified annuli. □

8 Explicit examples

Let us consider some examples of graph manifolds for which we will give a Heegaard splitting. These examples come from links of normal surface singularities.

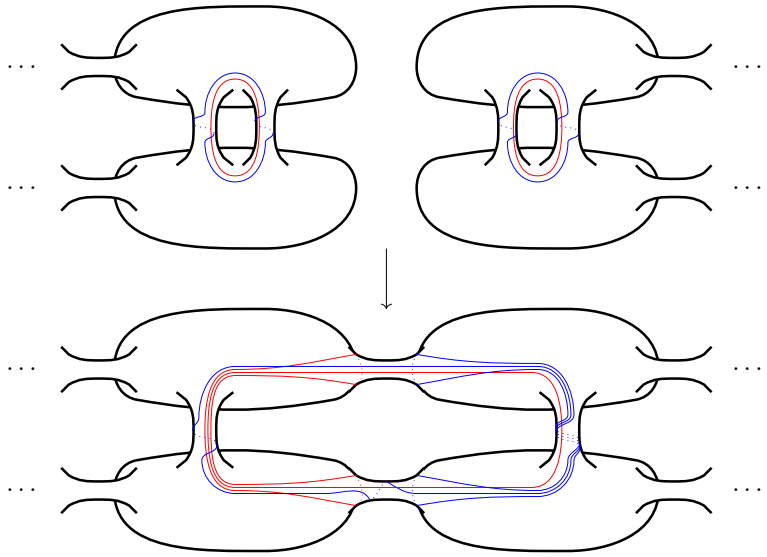

Fig. 18 Float gluing that closes a cycle

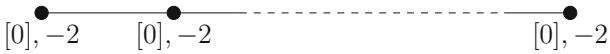

Fig. 19 $\mathbb{A}_n$ graph

Example 8.1 Let M be the link of the $\mathbb{A}_n$ singularity, a lens space $L(n, n-1)$. The graph of this manifold is a linear tree with $n-1$ vertices with $([0], -2)$ decorations.

With our method we obtain a genus 1 Heegaard splitting where the two curves intersect n times.

From now, we will drop the genus weight if it vanishes.

Example 8.2 Let us consider the plumbing manifold associated with a graph with one vertex and Euler number $-n$, link of a quotient singularity, i.e., the lens space $L(n, 1)$. With our method, we obtain a Heegaard splitting of genus $n-1$. Using Neumann plumbing calculus (namely $(n-1)$ $+1$-blowups and one -1-blowdown), we can transform it in the graph of Fig. 19, where the weights equal 2. The Heegaard splitting coincides with the one from the previous example, with a reversed orientation (Fig. 20).

Example 8.3 The plumbing manifold of Fig. 21 is also a lens space $L(5, 2)$ and it admits a Heegaard splitting of genus 1. However, our method provides a genus-2 Heegaard splitting (Fig. 22).

Example 8.4 The link of the singularity defined by $z^2 + x^3 + y^5 = 0$ ($\mathbb{E}_8$-singularity) is the Poincaré sphere. Our method provides a Heegaard splitting of genus 3, where the central vertex needs four drills (three negative ones).

It is possible to make a simpler Heegaard splitting. Using $+1$-blowups of [5] (and one -1-blowdown), we can modify the Euler numbers: 2 for the lower vertex and -1 in the central vertex. In that case, we can make a float gluing along the main cylinder, obtaining a Heegaard splitting of genus 2 (Fig. 23).

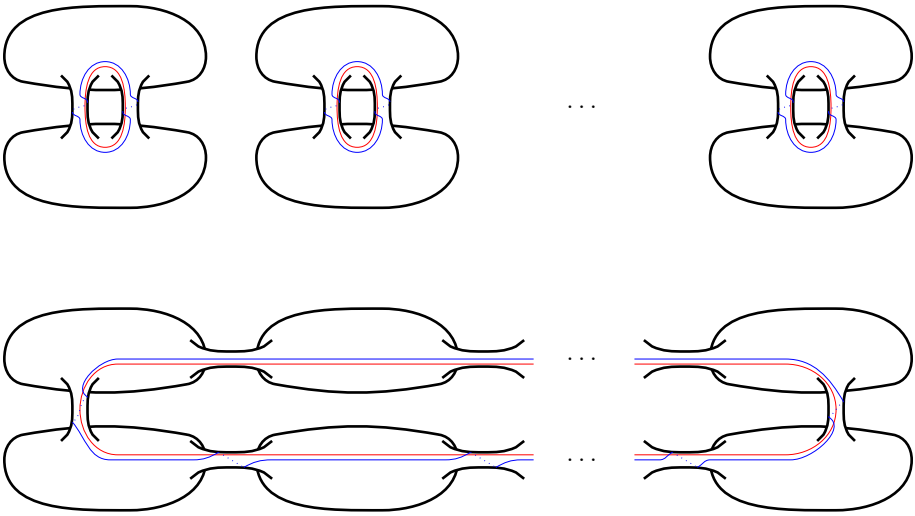

Fig. 20 Heegaard diagram of the $\mathbb{A}_n$ graph

Fig. 21 A quotient singularity

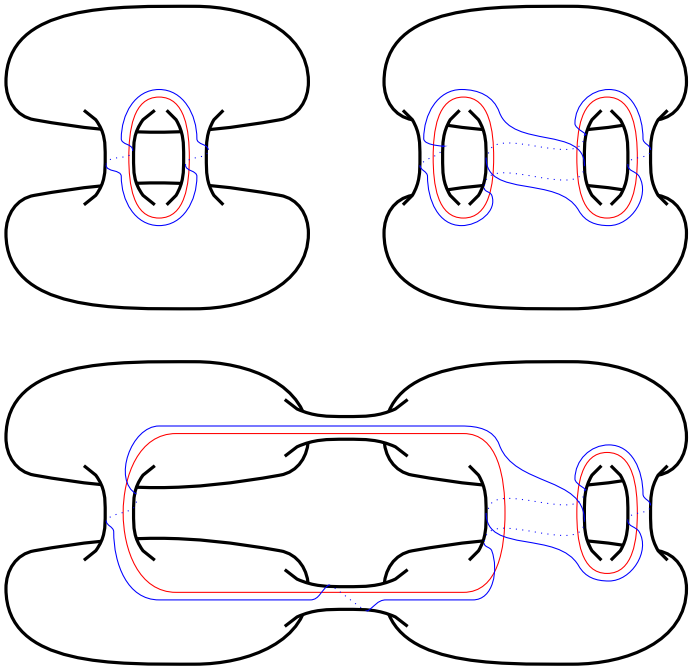

Fig. 22 Heegaard diagram of the quotient singularity

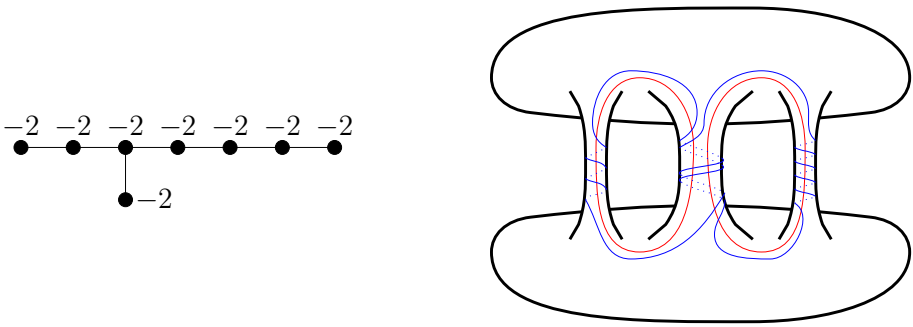

Fig. 23 Heegaard diagram of the $\mathbb{E}_8$-singularity

References

1. Boileau, M., Otal, J.-P.: Scindements de Heegaard et groupe des homéotopies des petites variétés de Seifert. Invent. Math. **106**(1), 85–107 (1991)
2. Boileau, M., Zieschang, H.: Heegaard genus of closed orientable Seifert 3-manifolds. Invent. Math. **76**(3), 455–468 (1984)
3. Heegaard, P.: Sur l' "Analysis situs". Bull. Soc. Math. Fr. **44**, 161–242 (1916)
4. Moriah, Y., Schultens, J.: Irreducible Heegaard splittings of Seifert fibered spaces are either vertical or horizontal. Topology **37**(5), 1089–1112 (1998)
5. Neumann, W.D.: A calculus for plumbing applied to the topology of complex surface singularities and degenerating complex curves. Trans. Am. Math. Soc. **268**(2), 299–344 (1981)
6. Ozsváth, P., Szabó, Z.: Holomorphic disks and three-manifold invariants: properties and applications. Ann. Math. (2) **159**(3), 1159–1245 (2004)
7. Ozsváth, P., Szabó, Z.: Holomorphic disks and topological invariants for closed three-manifolds. Ann. Math. (2) **159**(3), 1027–1158 (2004)
8. Rolfsen, D.: Knots and Links, Mathematics Lecture Series, vol. 7. Publish or Perish Inc., Berkeley (1970)
9. Sarkar, S., Wang, J.: An algorithm for computing some Heegaard Floer homologies. Ann. Math. (2) **171**(2), 1213–1236 (2010)
10. Schultens, J.: Heegaard splittings of graph manifolds. Geom. Topol. **8**, 831–876 (2004)
11. Waldhausen, F.: Eine klasse von 3-dimensionalen mannigfaltigkeiten I. Invent. Math. **3**, 308–333 (1967)
12. Waldhausen, F.: Eine klasse von 3-dimensionalen mannigfaltigkeiten II. Invent. Math. **4**, 87–117 (1967)